*Progress In Electromagnetics Research Letters, Vol. 105, 33–39, 2022*

# Compact Wideband Power Divider Based on Unequal-Width Three-Coupled-Lines

**Hongmei Liu*, Yihan Ma, Siran Zhang, Shaojun Fang, and Zhongbao Wang**

**Abstract**—In the paper, a compact wideband power divider (PD) which consists of a $\lambda/4$ unequal width three-coupled lines, four short-circuited stubs, and an airbridge resistor is presented. By connecting the four short-circuited stubs to the input and output ports of the PD, two additional transmission poles are obtained, which results in enhanced bandwidth and improved selectivity. Rigorous design equations are given according to the even-odd mode analysis, and the design parameters are obtained based on particle swarm optimization. For validation, a prototype operating at 1 GHz is fabricated and tested. The experimental results indicate that the proposed power divider exhibits a return loss of more than 17.5 dB and an isolation of larger than 18.8 dB isolation in the fractional bandwidth of 91%.

## 1. INTRODUCTION

Power divider (PD) which splits and combines power signal is widely used in RF and microwave systems. As a classic structure, Wilkinson power divider (WPD) [1] plays a major role due to its perfect impedance matching and isolation performance. In recent years, with the increasing transmission rate requirements of wireless communication systems, the research on wideband WPDs is a hotspot.

For wideband realization, the most common design method is cascading multi-section WPDs [2, 3]. In [2], the design of a WPD based on a cascaded structure to expand the bandwidth is firstly proposed by Cohn. Although the technique is effective, the size of the WPD is increased rapidly. In [3], by combining multi-section coupled lines with short-circuited stubs, an ultra-wideband (UWB) bandpass WPD with 63% fractional bandwidth (FBW) is presented. However, since at least three segments are cascaded, the size is large. For further bandwidth improvement, techniques such as connecting $\lambda/4$ impedance conversion line [4] or open-end parallel coupling line [5] are reported. But the problem of size reduction is not solved. In order to reduce the size, capacitors are introduced to shorten the electrical length of transmission line [6]. The total length of $\lambda/4$ is achieved with the FBW of 100%. However, the use of capacitors limits the operation frequency of the PD, and fabrication complexity is increased by the defected ground structure. Except multi-section cascading, methods of inserting additional transmission poles can also be used for wideband design, for example, open-circuit stub [7, 8], resonator [9, 10], and transversal signal-interference sections [11]. However, the influence of the size increase caused by introducing of above structures cannot be ignored.

Recently, three coupled lines (TCLs) [12–14] which have the features of multiport and wideband characteristics is preferred in the design of PD. In [12], a wideband PD with tunable power division ratio is proposed with small size, but the return loss is needed to be improved. Based on the equal-width TCLs and one short-circuit stub, a UWB PD is designed [13]. Unfortunately, no complete design formula is given. In [14], by replacing the T-junction in WPD with two TCLs, the FBW of 82.6% is obtained with a sharp selectivity. However, since equal-width TCL is adopted in [13] and [14], the performance of matching and isolation is deteriorated. Microstrip-to-slotline transitions based on single-layer [15],

*Received 26 May 2022, Accepted 24 June 2022, Scheduled 18 July 2022*
* Corresponding author: Hongmei Liu (lhm323@dlmu.edu.cn).
The authors are with the School of Information Science and Technology, Dalian Maritime University, Dalian, Liaoning 116026, China.

multi-layers [16], and integrated passive device technology [17] are also the effective methods to realize wideband PD. But the structure is complex. Despite the above studies, it is still a challenge to design a compact wideband power divider with good matching and isolation.

In this paper, a wideband PD based on unequal-width TCL is proposed with the advantage of good matching, isolation and compact size. The detailed analysis process and complete design formula are given in Section 2. For verifying the design method, a prototype operates at 1 GHz was fabricated and tested in Section 3. Finally, a concise conclusion is expressed in Section 4.

## 2. THEORETICAL ANALYSIS

The proposed compact wideband PD consists of $\lambda/4$ unequal-width TCLs, four short-circuited stubs, and one airbridge resistor, as shown in Fig. 1. Due to the symmetry of the circuit, when the power flows into port 1, the energy can be evenly coupled to the two sidelines (A-line) and then outputs at port 2 and port 3, respectively. Four short-circuited stubs which are connected to the input and output ports can obtain two additional transmission poles. Thus, the bandwidth of the PD is widened, and the selectivity of the passband edge is improved. Good isolation is also achieved by the resistor.

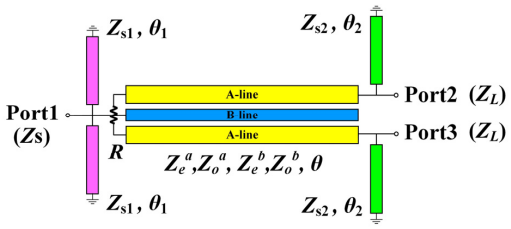


**Figure 1.** Schematic of proposed wideband PD.

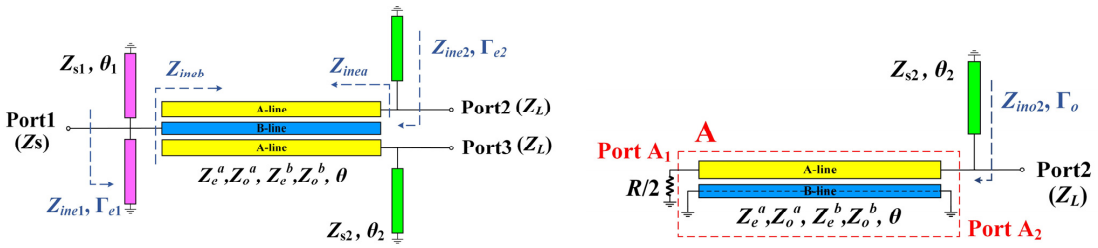


**Figure 2.** The equivalent circuit of (a) even-mode, (b) odd-mode.

The proposed PD can be analyzed by even-odd mode technique. When the excitation is even-mode, the voltage of the signals passing through ports 2 and 3 are in phase with the same amplitude. Fig. 2(a) shows the even-mode equivalent circuit of the proposed PD. According to the theoretical analysis of TCL in [18], the input impedance and reflection coefficient in Fig. 2(a) can be deduced as:

$$Z_{inea} = Z_1 + Z_7 - \frac{2Z_6^2}{Z_2 + \mathrm{j}Z_s Z_{s1}\tan\theta_1/(2Z_s + \mathrm{j}Z_{s1}\tan\theta_1)} \tag{1a}$$

$$Z_{ineb} = Z_2 - \frac{2Z_6^2}{Z_1 + Z_7 + \mathrm{j}Z_L Z_{s2}\tan\theta_2/(Z_L + \mathrm{j}Z_{s2}\tan\theta_2)} \tag{1b}$$

$$Z_{ine1} = \mathrm{j}\frac{Z_{ineb}Z_{s1}\tan\theta_1}{2Z_{ineb} + \mathrm{j}Z_{s1}\tan\theta_1} \tag{1c}$$

$$Z_{ine2} = \mathrm{j}\frac{Z_{ina}Z_{s2}\tan\theta_2}{Z_{ina} + \mathrm{j}Z_{s2}\tan\theta_2} \tag{1d}$$

$$\Gamma_{e1} = \frac{Z_{ine1} - Z_s}{Z_{ine1} + Z_s} \tag{2a}$$

$$\Gamma_{e2} = \frac{Z_{ine2} - Z_L}{Z_{ine2} + Z_L} \tag{2b}$$

where $Z_S$ and $Z_L$ represent the impedances of port 1 and port 2 (port 3), respectively. In the above equations, $Z_1$ and $Z_2$ are the self-impedances of A-line and B-line, respectively, $Z_3$, $Z_4$, $Z_5$, and $Z_6$ represent the cross impedance between the adjacent lines (A-line and B-line). $Z_7$ and $Z_8$ denote the cross impedances between two nonadjacent A-lines [18], as shown in (3).

$$\begin{cases} Z_1 = -\mathrm{j}\dfrac{(Z_e^a + Z_o^a)}{2}\cot\theta \\ Z_2 = -\mathrm{j}\dfrac{(Z_e^b + Z_o^b)}{2}\cot\theta \\ Z_3 = -\mathrm{j}\dfrac{(Z_e^a - Z_o^a)}{2}\cot\theta \\ Z_4 = -\mathrm{j}\dfrac{(Z_e^a + Z_o^a)}{2}\csc\theta \\ Z_5 = -\mathrm{j}\dfrac{(Z_e^b + Z_o^b)}{2}\csc\theta \\ Z_6 = -\mathrm{j}\dfrac{(Z_e^a - Z_o^a)}{2}\csc\theta \\ Z_7 = -\mathrm{j}\dfrac{K(Z_e^a - Z_o^a)}{2}\cot\theta \end{cases} \tag{3}$$

Here, the coupling coefficient ratio $K$ is set as 0.5.

When the circuit is in odd-mode excitation, the voltages of equal-amplitude with inverted phases are loaded at port 2 and port 3, respectively. Fig. 2(b) shows the odd-mode equivalent circuit. The impedance matrix of the two ports network A in the red dashed box and the input impedance can be expressed as:

$$\begin{cases} Z_{A11} = Z_{A22} = Z_1 + \dfrac{2Z_3Z_5Z_6 - Z_2(Z_3^2 + Z_6^2)}{Z_2^2 - Z_5^2} \\ Z_{A12} = Z_{A21} = Z_4 + \dfrac{Z_5(Z_3^2 + Z_6^2) - 2Z_2Z_3Z_6}{Z_2^2 - Z_5^2} \end{cases} \tag{4a}$$

$$Z_{ino2} = \mathrm{j}\frac{(Z_{A22}(R/2 + Z_{A11}) - Z_{A12}Z_{A21}) \cdot Z_{s2}\tan\theta_2}{(Z_{A22} + \mathrm{j}Z_{s2}\tan\theta_2)(R/2 + Z_{A11}) - Z_{A12}Z_{A21}} \tag{4b}$$

$$\Gamma_o = \frac{Z_{ino2} - Z_L}{Z_{ino2} + Z_L} \tag{5}$$

Then, the $S$-parameters of proposed compact wideband PD can be given as:

$$S_{11} = S_{11,e} = \Gamma_{e1} \tag{6a}$$

$$S_{21} = S_{31} = \frac{S_{21,e}}{\sqrt{2}} \tag{6b}$$

$$S_{22} = S_{33} = \frac{\Gamma_{e2} + \Gamma_o}{2} \tag{6c}$$

$$S_{23} = S_{32} = \frac{\Gamma_{e2} - \Gamma_o}{2} \tag{6d}$$

In order to ensure that the proposed PD has good matching and isolation in the designed wide bandwidth, the $S$-parameters in (6) are substituted into the particle swarm optimization (PSO) [19] to

obtain the optimized results. The objective function $F$ is defined as (7) and is expected to approach zero as much as possible.

$$F(Z_e^a, Z_o^a, Z_e^b, Z_o^b, Z_{s1}, Z_{s2}, R) = g_1 + g_2 + g_3 \tag{7a}$$

$$g_1 = \frac{1}{N}\sum_{i=1}^{N} |S_{11}(f_i)|^2 \tag{7b}$$

$$g_2 = \frac{1}{N}\sum_{i=1}^{N} |S_{22}(f_i)|^2 \tag{7c}$$

$$g_3 = \frac{1}{N}\sum_{i=1}^{N} |S_{23}(f_i)|^2 \tag{7d}$$

Here, $f_0$ is the center frequency of PD, and $f_i$ represents the sampling frequency which is defined as $f_i = f_0[1 + (i-1)/D]$ $(i = 1, \ldots, N)$. $f_0/D$ is the sample interval, and $N$ is the number of sampling points. According to above analysis, the design process of the proposed compact wideband PD can be summarized into the following steps:

1) Determine the center frequency $f_0$ and FBW. Then appropriate sample interval $f_0/D$ and sampling point number $N$ are selected accordingly.
2) Based on the objective function $F$, the desired circuit impedance parameters and resistance value are obtained by PSO.
3) Build a compact microstrip circuit model of proposed PD, then full-wave simulation of the model is carried out in EM simulation tool, and the optimization parameters are slightly adjusted at the same time.
4) Fabricate and measure a prototype to prove the feasibility of the design program.

## 3. DESIGN AND IMPLEMENTATION

To verify the proposed structure and design method, a PD operating at 1 GHz with 20 dB return loss (RL) and isolation (IO) in 100% FBW is designed. According to the design goals, the values of $D$ and $N$ are set as 20 and 11, and the frequency range is defined as $0.5 \sim 1.5$ GHz. Here, $\theta = \theta_1 = \theta_2 = \pi/2$. After optimization using PSO, the impedance parameters are $Z_e^a = 107\,\Omega$, $Z_o^a = 30.2\,\Omega$, $Z_e^b = 127.4\,\Omega$, $Z_o^b = 50.6\,\Omega$, $Z_{s1} = 145.3\,\Omega$ and $Z_{s2} = 136.6\,\Omega$, and $R = 122.5\,\Omega$. Fig. 3 shows the corresponding theoretical calculated $S$-parameters. It can be seen that within 100% FBW, the RL and IO are greater than 20 dB which meets the design index.

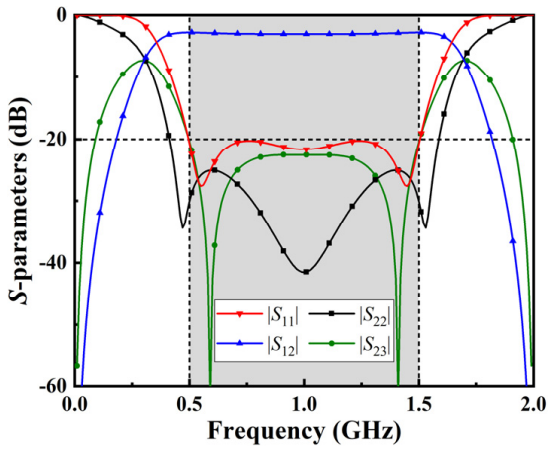


**Figure 3.** Theoretical calculation $S$-parameters of the proposed wideband PD.

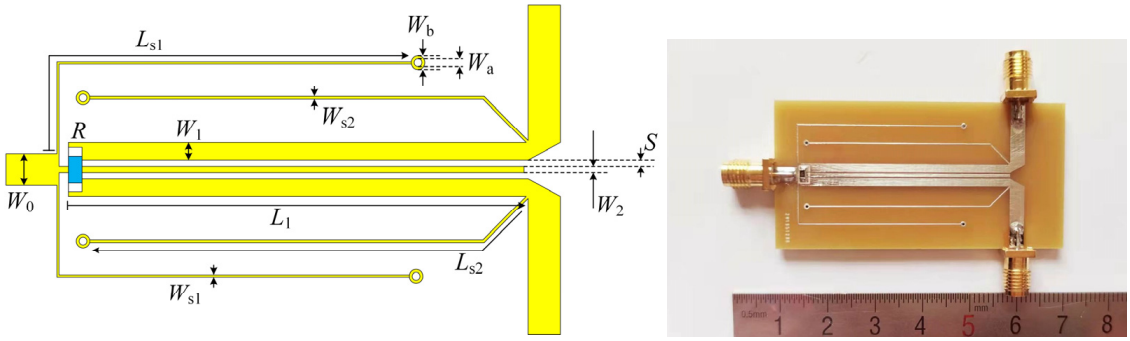


**Figure 4.** (a) Layout and (b) photograph of the fabricated wideband PD.

Further, using the dielectric substrate made of FR-4 ($\varepsilon_r = 4.4$, $\tan\delta = 0.02$, $h = 1.524\,\text{mm}$), the circuit model is established in the HFSS (commercial EM analysis tool) for simulation and appropriate adjustment. Fig. 4 shows the layout and photograph of the fabricated wideband PD with an overall size of 30 mm × 60 mm. The size regardless of the input/output feed lines is $0.13\lambda_g \times 0.27\lambda_g$. The corresponding physical dimensions are $W_0 = 3\,\text{mm}$, $W_1 = 1.6\,\text{mm}$, $W_2 = 0.7\,\text{mm}$, $W_{s1} = 0.2\,\text{mm}$, $W_{s2} = 0.26\,\text{mm}$, $L_1 = 43.3\,\text{mm}$, $L_{s1} = 44\,\text{mm}$, $L_{s2} = 44\,\text{mm}$, $S = 0.2\,\text{mm}$, $W_a = 0.6\,\text{mm}$, $W_b = 1.2\,\text{mm}$. The value of airbridge resistor $R$ is $120\,\Omega$. And it is connected on the two A-lines of the TCLs.

Figure 5 shows the simulated and measured $S$-parameters of the fabricated prototype. It is observed that in the simulated FBW of 100%, the input and output RLs are more than 18.4 dB and 20.5 dB, respectively. And the IO is larger than 21.7 dB with an insertion loss (IL) of less than 0.4 dB. Good frequency selectivity at $2f_0$ is also obtained. Measurement results are in good agreement with simulation. In the range of 0.53 to 1.44 GHz (FBW = 91%), the measured input RL is better than 17.5 dB with less than 1.3 dB IL. While the in-band IO and output RLs are both greater than 18.8 dB. Fig. 6 shows the measured phase and magnitude imbalance between ports 2 and 3. The measured magnitude and phase differential are ±0.3 dB and ±0.4°, respectively. Taking the simulated results as a reference, the measured $S$-parameters are shifted to lower frequency which may be caused by the dielectric constant deflection and manufacturing deviation. Table 1 shows the comparison between the proposed wideband PD and the representative works in recent years. It can be intuitively found that the design structure in this paper has some advantages of wide bandwidth, better matching, good isolation, and smaller size.

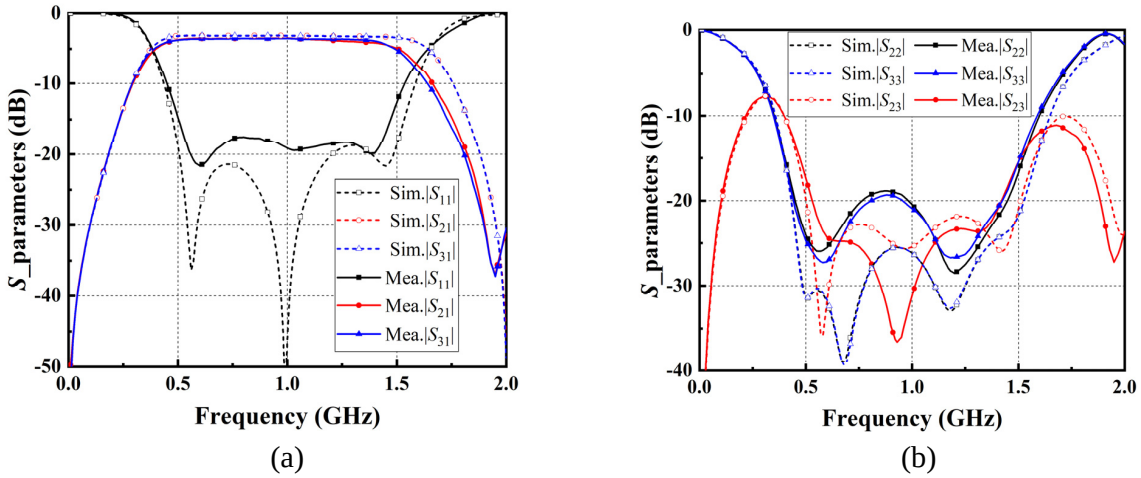


**Figure 5.** Simulated and measured $S$-parameters. (a) $|S_{11}|$, $|S_{21}|$ & $|S_{31}|$. (b) $|S_{22}|$, $|S_{33}|$ & $|S_{23}|$.

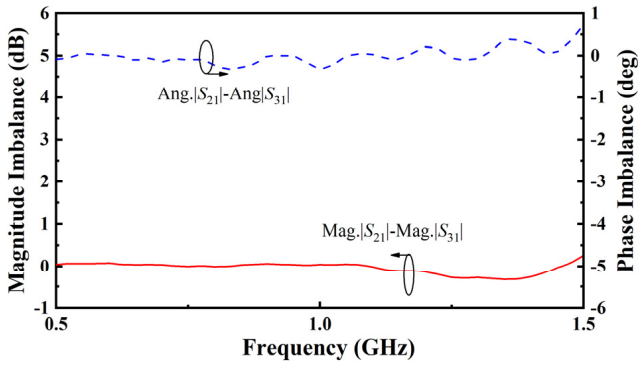


**Figure 6.** Measured phase and magnitude imbalance.

**Table 1.** Performance comparison between proposed and published wideband PD.

| Ref. | Input RL (dB) | Output RL (dB) | IL (dB) | FBW | IO. | NLE. | Technology | Size ($\lambda_g \times \lambda_g$) |
|---|---|---|---|---|---|---|---|---|
| [3] | 21.1 | 19.2 | – | 63% | 18.5 | 3 | Microstrip | $0.18 \times 0.56$ |
| [4] | 10 | 10 | 0.3 | 100% | 15 | 3 | Microstrip | $0.11 \times 0.67^*$ |
| [6] | 20 | 20 | 0.47 | 101% | 20 | 9 | Microstrip with DGS | $- \times 0.25$ |
| [8] | 15 | 13* | – | 70% | 16.7 | 1 | Microstrip | $0.29 \times 0.4$ |
| [9] | 10 | 10 | 0.7 | 78% | 17.5 | 1 | Microstrip | $0.31 \times 0.74$ |
| [11] | 15 | 15 | – | 90% | 17 | 3 | Microstrip | $0.5 \times 0.8$ |
| [14] | 12 | 12 | 0.8 | 82.6% | 23 | 1 | Microstrip | $0.05 \times 0.32$ |
| [15] | 11 | 11.5 | 2 | 110% | 13 | 1 | Microstrip to slotline | $0.86 \times 1.08^*$ |
| [16] | 10 | 10 | 2 | UBW | 10 | 1 | Multilayer Microstrip to slotline | – |
| This work | 17.5 | 18.8 | 1.3 | 91% | 18.8 | 1 | Microstrip | $0.13 \times 0.27$ |

Iso.: Isolation. NLE.: Number of lumped elements. DGS: Defected ground structure.
UBW: Ultra-wideband. *: Means the data not been given but can be obtained indirectly.

## 4. CONCLUSION

A PD with the features of wideband and compact size is proposed in the paper. By combing unequal-width TCLs with four short-circuited stubs and one resistor, wideband operation with good impedance matching and isolation is achieved. The measurement results show that an FBW of 91% is realized with 17.5 dB RL and 18.8 dB IO, which is suitable for modern wireless communication systems.

## ACKNOWLEDGMENT

This work was supported in part by the National Natural Science Foundation of China under Grant 51809030 and Grant 61871417, in part by the Liaoning Revitalization Talents Program under Grant XLYC2007067, in part by the Dalian Youth Science and Technology Star Project under Grant 2020RQ007 and in part by the Fundamental Research Funds for the Central Universities under Grant 3132022245.

## REFERENCES


1. Wilkinson, E. J., "An N-way hybrid power divider," *IRE Trans. on Microwave Theory and Techniques*, Vol. 8, No. 1, 116–118, Jan. 1960.
2. Cohn, S. B., "A class of broadband three-port TEM-mode hybrids," *IEEE Trans. on Microwave Theory and Techniques*, Vol. 16, No. 2, 110–116, Feb. 1968.
3. Bao, C., X. Wang, Z. Ma, C. P. Chen, and G. Lu, "An optimization algorithm in ultrawideband bandpass Wilkinson power divider for controllable equal-ripple level," *IEEE Microwave and Wireless Components Letters*, Vol. 30, No. 9, 861–864, Sep. 2020.
4. Ahmed, U. and A. Abbosh, "Compact power divider for wideband in-phase and out-of-phase performances using parallel coupled lines," *Electronics Letters*, Vol. 53, No. 19, 1312–1314, 2017.
5. Maktoomi, M. A., M. S. Hashmi, and F. M. Ghannouchi, "Theory and design of a novel wideband DC isolated Wilkinson power divider," *IEEE Microwave and Wireless Components Letters*, Vol. 26, No. 8, 586–588, Aug. 2016.
6. Yu, T., "A broadband Wilkinson power divider based on the segmented structure," *IEEE Trans. on Microwave Theory and Techniques*, Vol. 66, No. 4, 1902–1911, Apr. 2018.
7. Wong, S. W. and L. Zhu, "Ultra-wideband power divider with good in-band splitting and isolation performances," *IEEE Microwave and Wireless Components Letters*, Vol. 18, No. 8, 518–520, Aug. 2008.
8. Zhang, B. and Y. A. Liu, "Wideband filtering power divider with high selectivity," *Electronics Letters*, Vol. 51, No. 23, 1950–1952, Nov. 2015.
9. Liu, Y., L. Zhu, and S. Sun, "Proposal and design of a power divider with wideband power division and port-to-port isolation: A new topology," *IEEE Trans. on Microwave Theory and Techniques*, Vol. 68, No. 4, 1431–1438, Apr. 2020.
10. Chen, M. T. and C. W. Tang, "Design of the filtering power divider with a wide passband and stopband," *IEEE Microwave and Wireless Components Letters*, Vol. 28, No. 7, 570–572, Jul. 2018.
11. Jiao, L., Y. Wu, Y. Liu, Q. Xue, and Z. Ghassemlooy, "Wideband filtering power divider with embedded transversal signal-interference sections," *IEEE Microwave and Wireless Components Letters*, Vol. 27, No. 12, 1068–1070, Dec. 2017.
12. Guo, L., H. Zhu, and A. M. Abbosh, "Wideband tunable in-phase power divider using three-line coupled structure," *IEEE Microwave and Wireless Components Letters*, Vol. 26, No. 6, 404–406, Jun. 2016.
13. Dang, T. S., C. W. Kim, and S. W. Yoon, "Ultra-wideband power divider using three parallel-coupled lines and one shunt stub," *Electronics Letters*, Vol. 50, No. 2, 95–96, Jan. 2014.
14. Xu, K. D., Y. Bai, X. Ren, and Q. Xue, "Broadband filtering power dividers using simple three-line coupled structures," *IEEE Trans. on Components, Packaging and Manufacturing Technology*, Vol. 9, No. 6, 1103–1110, Jun. 2019.
15. Zhu, H., Z. Cheng, and Y. J. Guo, "Design of wideband in-phase and out-of-phase power dividers using microstrip-to-slotline transitions and slotline resonators," *IEEE Trans. on Microwave Theory and Techniques*, Vol. 67, No. 4, 1412–1424, Apr. 2019.
16. Song, K. and Q. Xue, "Novel ultra-wideband (UWB) multilayer slotline power divider with bandpass response," *IEEE Microwave and Wireless Components Letters*, Vol. 20, No. 1, 13–15, Jan. 2010.
17. Kong, M., Y. Wu, Z. Zhuang, W. Wang, and C. Wang, "Ultraminiaturized wideband Quasi-Chebyshev/-Elliptic impedance-transforming power divider based on integrated passive device technology," *IEEE Trans. on Plasma Science*, Vol. 48, No. 4, 858–866, Apr. 2020.
18. Liu, H., Y. Ma, M. Guan, S. Fang, and Z. Wang, "Synthesis of miniaturized wideband four-way filtering power divider consisting of unequal-width three-coupled-lines," *Int. J. RF Microw. Comput. Aided Eng.*, Vol. 31, No. 10, e22805, Oct. 2021.
19. Muraguchi, M., T. Yukitake, and Y. Naito, "Optimum design of 3-dB branch-line couplers using microstrip lines," *IEEE Trans. on Microwave Theory and Techniques*, Vol. 31, No. 8, 674–678, Aug. 1983.